Investigation of Creep Behavior of CNT Reinforced Ti6Al4V Under Dynamic Loads

[1]Ismail Topcu*, [2]Burcu Nilgün Çetiner, [2] Arif N. Güllüoğlu and [3]Özkan Gülsoy
[1]Alanya Alaaddin Keykubat University, Engineering Faculty, Metallurgy & Materials Eng. Dept., 07752 Alanya, Antalya-Turkey.
[2]Marmara University, Engineering Faculty, Metallurgy & Materials Eng. Dept.,34722, Göztepe, İstanbul-Turkey.
[3]Marmara University, Technology Faculty, Metallurgy & Materials Eng. Dept.,34722, Göztepe, İstanbul-Turkey.
ismail.topcu@alanya.edu.tr*

(Received on 28th March 2019, accepted in revised form 28th March 2019)

Summary: This study investigates the effects of addition of Carbon nanotube (CNT) at different volume ratios (0.5- 5%) into Ti6Al4V matrix by mechanical alloying in terms of the density, microstructure, hardness and creep under dynamic load. As a result of the good bonding of carbon nanotubes powders with the main matrix, Ti-6Al-4V/CNT composites have experienced change both in microstructure and mechanical properties (such as hardness, density) and, correspondingly, qualitatively creep behaviour of Ti-6Al - 4V matrix alloy has been improved compared to the lean one. The density of CNT reinforced Ti6Al4V composites sintered at 1300°C for 3h decreases with increasing CNT content. The hardness tests indicated that the hardness of composites increased with CNT addition. In addition, although creep strain is decreased continually with CNT content until 5%, creep life increased with increasing CNT content until 4% of CNT but decreased above 4%. After sintering at 1300 °C under vacuum for 3 hours the density of the composite material reached to a level of 98.5 %, the microhardness to 538 HV and the creep behaviour was improved. The characterization of Ti6Al4V / CNT composites after mechanical alloying was carried out using scanning electron microscopy (SEM), energy dispersive x-rays spectroscopy (EDS) analysis and X-ray diffraction (XRD) methods.

Although Ti–6Al–4V alloys are used as biomaterial, this study aimed at using MWCNTs containing Ti-6Al-4V composites at high temperature applications. Because MWCNTs reinforced Ti-6Al-4V composites are cheaper and have lower weight than the other materials used in this kind of applications.

Keywords: Dynamic creep, Carbon nanotubes, Sintering, Ti6Al4V.

Introduction

The aerospace, automotive and biomedical industries are some of viadly used fields where titanum alloys have been used. Because of its heat treatment capability, good mechanical strength, high corrosion resistance and biocompatibility, Ti–6Al–4V alloy containing 6 wt.% Al (Aluminum), 4 wt.% V (Vanadium) and Ti (Titanium); balance, has been used in airplane turbines and medical implants [1, 2].

The requirement of high strength, lightweight and fuel-efficient materials in automotive and aerospace industries provides a big research interest [3, 4]. Mechanical and corrosion resistance charecteristics of Titanium (Ti) and alloys, which have high specific strength and low specific gravity, makes them highly relavant to these industries [5,6]. Because of its superiror mechanical performance in service, Ti-6Al-4V alloy has been widely preferred in the aerospace industry and constitutes 45 % of the total Ti production [7-9]. Although Ti-6Al-4V has important characteristics that make it a good candidate for the aerospace industry, the production of the alloy is a major drawback due to the high affinity to the nitrogen and oxygen during the process. So, it can endanger the ductility property [10]. Therefore, processing of Ti-6Al-4V under vacuum atmospheres at high temperatures is a key requirement unless the properties of the bulk material are put at risk by interstitial elements [11]. This necessity results in very expensive process and limits the application of Ti-6Al-4V products. Composite materials reinforced with Multi-walled carbon nanotubes (MWCNTs) have made great progress and experience a few distinctive applications by the advanteges of mechanical, electrical and thermal properties. [8-12]. Due to their extremely higy strength, MWCNTs are used as reinforcement element for the composite materials. In addition, the multi walled carbon nanotubes maintain good dispersion strengthening of composite materials [13-16]. The reinforcement of metal matrix composites can alter the mechanical properties of the composites;

***To whom all correspondence should be addressed.**

hence their applications can broaden. Since titanium carbide (TiC) was compatible with the titanium alloys, it has been used for the reinforcement to date [17-20]. But, the studies on MWCNTs reinforced MMC and CMC materials are restricted. Hot pressing and high sintering temperature methods have been used to produce MWCNTs reinforced Ceramic Matrix Composites materials [21-23]. Recent studies have proposed that MWCNTs is an ideal candidate for the ultra-high strength reinforcements [24]. MWCNTs, which has a low density, is used as an exquisite reinforcement against friction for metal matrices due to extraordinary physical properties. Nevertheless, number of reports in this field is limited due to challenges during the processing of MWCNTs [25-27]. Creep measurements of a titanium component are not easy because of its entire creep life which can reach up to 120000 hours [28]. However, short-term creep tests are widely preferred [29, 30]. Hence, it has been carried out short-term creep tests of alloys.

In this research, it was aimed to produce a novel material to be used under high temperature, loads and stresses with potential of possible applications in aero-space industry.

Experimental

In this study, Ti–6Al–4V and MWCNTs powders were used as the starting materials. Gas atomised Ti-6Al-4V powders provided by Phelly Materials Company have spherical shape and homogenous without agglomeration. The average particle size of MWCNTs powders were about 10-30 nanometers. Different volume percentage of MWCNTs (0.5 to 5 v/v%) were dispersed into Ti-6Al-4V powders inside glass containers (inner diameter: 40 mm, capacity: 100 ml) and mixed with the help of a turbula ball mill (Turbula PM 400 MA, Switzerland) using alumina balls of same sizes (diamaeter: 7 mm, weight ratio: 1:6:1). Using same size of milling balls during the process makes sure that sufficient collision energy is provided to the powder particles [3, 31, 32]. A binder system consisting of poliacrilonitril (PAN) was used. This process was prepared at first and then powder blend added incrementally. The powder loading in this mixture was 98.5 vol. percentages. Creep specimens were uniaxial pressed using a 300 MPa moulding machine.

Samples were sintered at 1300 °C by heating rate of 10 ° C/min under 10^{-6} Torr under vacuum for 3 hours [33]. In order to avoid the oxidation of both Ti alloy and CNT powders, the sintering was performed under high vacuum atmosphere. The Archimedes water immersion method was applied in order to determine the densities of the sintered samples were measured by means of the Archimedes water immersion method. The specimens were cut by abrasive cutter from their centers before metalllographic examination, then ground and polished. As etchant, the Kroll reagent (1 or 2 part (s) of hydrofluoric acid, 2 or 3 parts of nitric acid in about 50 parts of distilled water) was selected for optical metallographic observation. All creep experiments were performed using Instron Model 8802 Creep tester with 100 Mpa dynamic stress and low frequency. In these experiments, cylindrical samples of 30 mm length and 10 mm diameter were used. The hardness tests were performed using a Future-Tech (FM-110) micro hardness test machine at HV scale. At least fifteen measurements were tested on the same specimen under the same conditions to guarantee the reliability of the results. XRD analysis was performed using CuKα radiation source and a graphite filter where the range was between 20° and 85° with a step of 0.05° and 1 s of counting time. The microstructure of the powder samples after sintering was examined using SEM (Jeol-JSM 6335F) after molding.

Results and Discussion

Characterization of powders produced

Gas atomised Ti-6Al-4V powders provided by Phelly Materials Company have spherical shape and they are characterised in terms of particle morphology and size using SEM in order to observe the structure of the starting powders (Ti-6Al-4V and MWCNTs) and the images are given in Fig.1. Ti-6Al - 4V powders' image is shown in Fig. 1a [26,27]. No agglomeration was observed in the samples. However, MWCNTs seen in Fig. 1b were - observed to be agglomerated [28]. The reason behind the agglomeration is attributed not only to the large surface area and high aspect ratio of MWCNTs powder but also as well as the collective and cooperative strong intermolecular bonding induced from the singular nanotubes [3, 34]. As a characteristic of gas-atomization process Ti-6Al-4V powders have spherical shape which is shown in Fig. 1a and there was no agglomeration. It has a particle size distribution of D10= 58, 27 μ, D50 =110, 65 μ, D90=171,39 μ with a density of 4.43 g/cm3 as raw material. MWCNTs reinforcement material was purchased by Cheep Tubes Company (USA), with a density of 2.31 g/cm3. Different than Ti-6Al-4V powders, MWCNTs were highly agglomerated and entangled as presented in Fig. 1b. Fig 2 gives the powder size distribution of the Ti–6Al–4V powder. Fig. 2 indicates that the powder has a particle size between 145-180 μm.

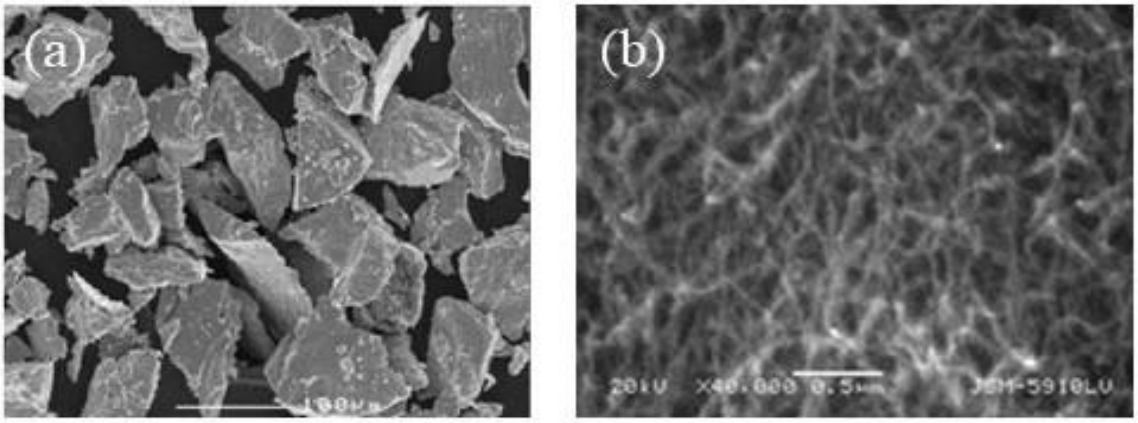

Fig. 1: SEM images of Ti-6Al-4V and MWCNT powders a) Ti-6Al-4V and b) MWCNT.

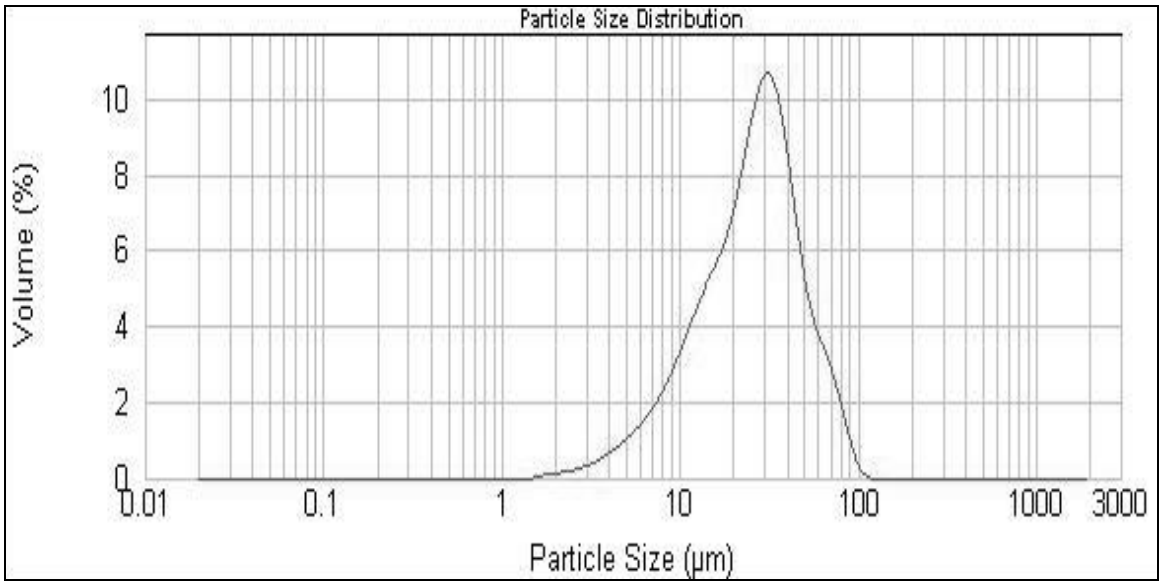

Fig. 2: Ti–6Al–4V Particle size distribution (Malvern Laser Particle Sizer; Hydro 2000).

The ratios of Ti - 6Al - 4V and MWCNT powders with different volumetric percentage (0.5-5%) were determined. These mixtures were obtained by mechanical alloying, 1 % binder into 100 ml glass jars with 10 mm diameter alumina balls were added. Backscatter image of the Ti-6Al-4V/MWCNTs powders after 5h of grinding by ball milling process is given in Fig. 3.

Different volume ratios of MWCNTs were dispersed as reinforcement in the matrix alloy and the homogenous dispersion of the reinforcement was dependent on the volume ratio: the possibility of achieving homogenous dispersion was less when the volume ratio of MWCNTs is higher. This is ascribed to the large surface area, high aspect ratio (with a length many times that of their width), powerful intermolecular bonding in the singular tubes and tubular morphology/nano size dimensions of the MWCNTs which are giving rise to clustering and agglomeration [3,35]. Therefore, a relatively homogenous distribution of the MWCNTs was obtained in the mixture having 1% MWCNTs. On the other hand, clusters and agglomeration of MWCNTs, which is depicted by elipses in Fig. 2, was noticed when the volume ratio is high. The dissipation of the MWCNTs in Ti-6Al-4V matrix was adequate with 4% volume ratio. This was considered due to the trouble in distributing MWCNTs within the metal main phase when their volume ratio is high which supports the explanation aferomentioned above. The XRD analysis of the pulverized mixtures for different volume ratio of MWCNTs are given in Fig. 4.

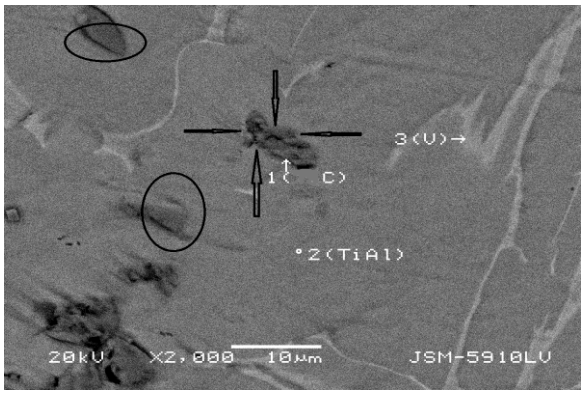

Fig. 3: Backscattering image of the composite material (TiC (1), (TiAl(2), V (3).

As a result of the XRD analysis of the composite powders produced, the increase in the peak intensity and the growth in the peak areas were significant. It is important to indicate that the presence of MWCNT in the structure causes some negativity and that it induces agglomerate distribution in the MWCNT based metal matrix implied by Cai *et al* [36].

The X-Ray diffractions of the samples having various MWCNTs contents are shown in Fig. 3 which shows the peaks at 2° of 38.44° and 44.7° belongs to the Ti6Al4V, and, MWCNTs peaks are observed at 25° and 53°. In addition, additional MWCNTs peak formed at 63.5° for the sixth sample that has 5% MWCNTs. Moreover, the intensity of the peaks showed an obvious enhancement depending on the MWCNTs ratio. In other words, that increasing MWCNTs contents cause an increase in the area of the main peaks of MWCNTs.

Characterization of the produced specimen materials

Microstructures of the plain Ti-6Al-4V and Ti-6Al-4V/MWCNTs reinforced composites after sintering at 1300 °C were investigated using SEM as shown in Fig. 5.

Equi-axed structures were obtained with the adition of MWCNTs to the Ti-6Al-4V as shown in Fig. 4. There was not any significant porosity in the microstructure which shows a good sintering behaviour. Samples with 4 and 5% volume of MWCNTs indicated re-agglomeration, depicted by white arrows in Fig. 5, and interfacial product of titanium carbide (TiC) was observed in the microstructure, indicated by black arrows in Fig. 5. Inadequate dispersion of the MWCNTs resulted in this re-agglomeration and it is promoted the interfacial reaction between MWCNTs and Ti-6Al-4V giving rise to formation of TiC. This situation is more noticeable for the samples having 5% volume MWCNTs where there are more clustered particles of TiC as MWCNTs in this sample were highly agglomerated into large clumps. It is believed that these clustered TiC particles were produced around the around the lump of MWCNTs which is also reported in other studies [3,37].

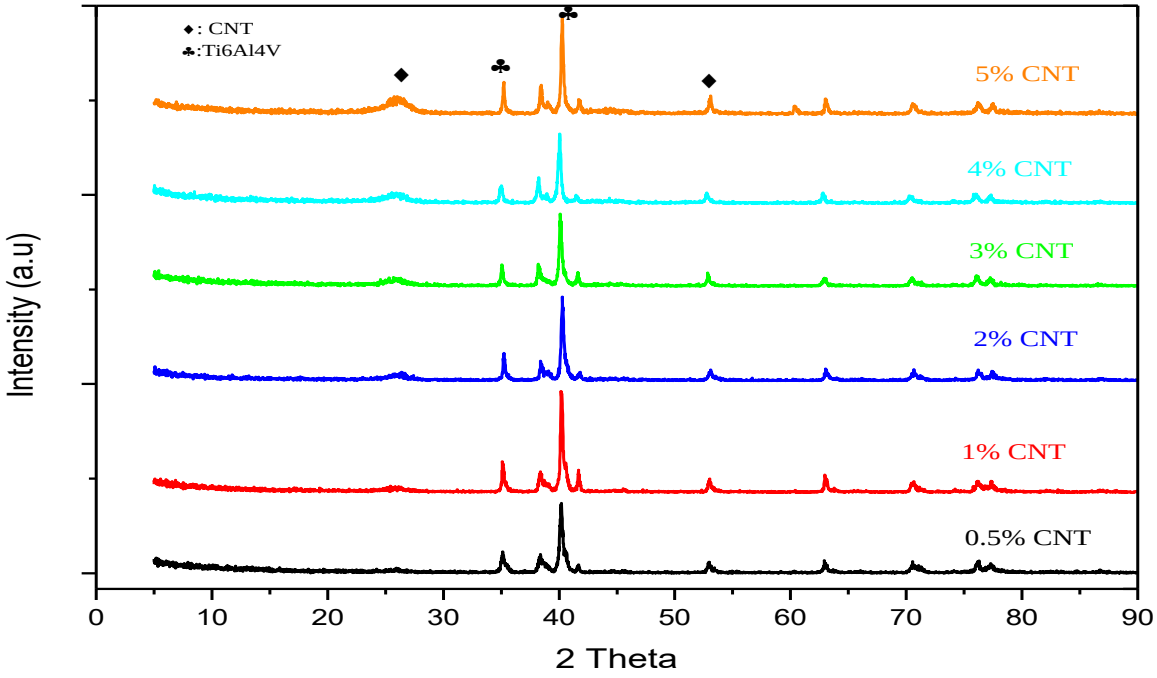

Fig. 4: XRD pattern of 5 % content MWCNTs particles in Ti–6Al–4V Matrix.

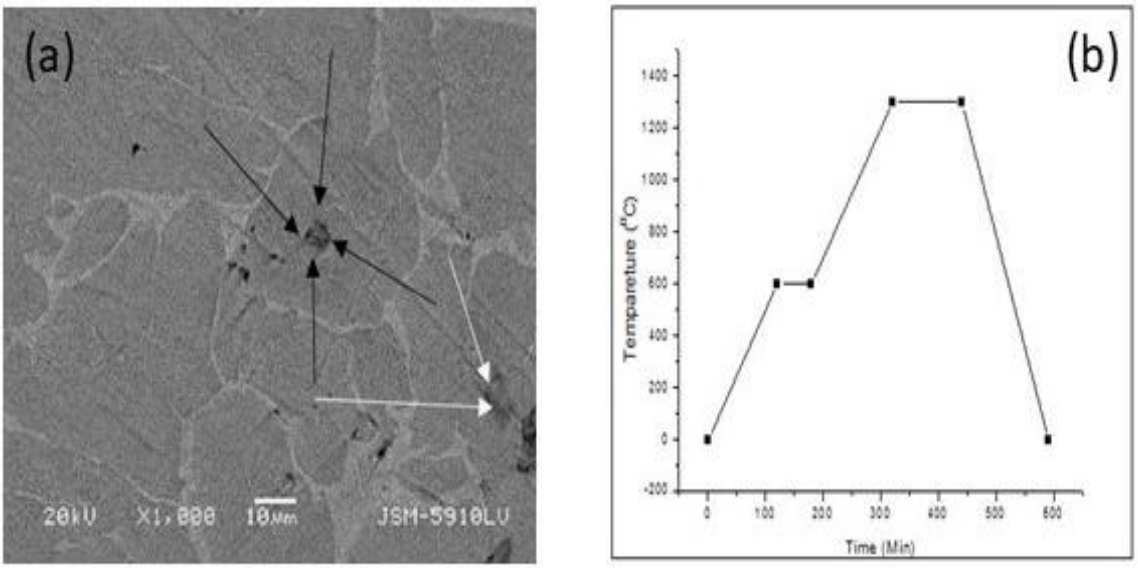

Fig. 5: (a) SEM image of Ti-6Al-4V/MWCNT composite, (b) Sintering process of 0.5-5 % content MWCNTs particles in Ti–6Al–4V Matrix.

Sample with 1% volume of MWCNT had a completely compact microstructure, also homogeneously dispersed α and β phases without any re-agglomeration and interfacial products which supports the adequate distribution of MWCNTs. The matrix phase (grey-colored) is α and the white strips like phase located on the grain boundaries is β as given in Fig. 6. The final evaluation of the microstructure (Alpha and beta) phases is given in the SEM micrograph of the sintered samples in Fig. 6. The reinforced Ti–6Al–4V alloy had only two phases of titanium (alpha and beta). Carbon structure was detected in the specimens with 4 and 5 volume % MWCNTs, respectively [3,38].

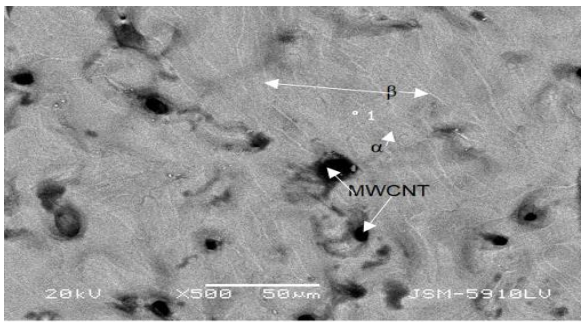

Fig. 6: SEM image of Ti-6Al-4V/MWCNT composite.

Effect of MWCNTs reinforced on the density of Ti-6Al-4V/MWCNTs composites

Archimedean density measurement results of the samples which were sintered at 1300 °C are given in Fig. 7 for different volume ratio of MWCNTs.

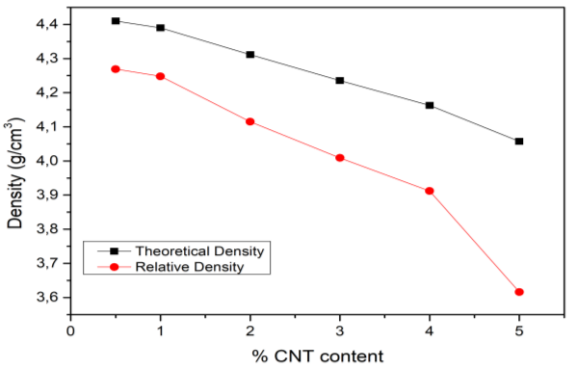

Fig. 7: CNT percentage reinforced by the density of different exchange rates.

Sintered density of Ti-6Al-4V/MWCNTs composites had a tendency of decreasing density by an increase in the MWCNTs ratio. This is most likely due to the clustering and aggloremation of the MWCNTs reinforcement in the matrix. Another reason for the decrease in the density might be insufficient diffusion between Ti-6Al-4V and MWCNTs which results in a weak interfacial bonding leading to thermal mismatch between the MWCNTs reinforcement and Ti-6Al-4V matrix. Better relative density obtained for the low MWCNTs content such as 1% volume was considered as a result of better homogenous dispersion of the reinforcement within the matrix [39].

It was previously discussed that [36] MWCNTs reinforced Al alloys and Ti matrices can

have a deterioration in the relative density of sintered bulk composite material with an increase in the MWCNTs ratio which supports the observation of this study. This deterioration in the density can be expected due to the higher possibility of pre-agglomeration and re-agglomeration which increases by an increment in the volume ratios of MWCNTs as mentioned previously.

Influence of MWCNTs reinforced on the microhardness of Ti-6Al-4V/MWCNTs composites

Microhardness measurement of the sintered plain Ti–6Al–4V and Ti–6Al–4V /MWCNTs reinforced samples were performed and the results are given in Fig. 8. It was shown that the hardness increases by the ratio of MWCNTs which is different than the density trend. The enhancement in microhardness with augmented high sintering temperature that was detected in the Ti–6Al–4V /MWCNTs composites was partially credited to the development of decreasing in pore volumes and intensification in density associated with elevated sintering temperature.

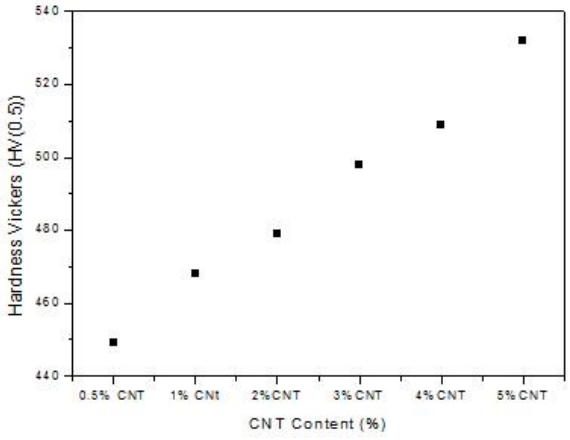

Fig. 8: The hardness versus different MWCNTs content (0.5- 5 %).

The reason for increase in hardness with MWCNTs content might be related to the hard interfacial product TiC which is more pronounced at higher volume % of MWCNTs. Additionally, another reason for the increase in hardness by adding more MWCNTs reinforcement can be the existence of retained MWCNTs as well as crystalline TiC hard phases [3, 38, 40]. Also as C atoms are miniscule compared to Ti atoms, they're placed in interatomic sites as interstitial atoms in the crystal lattice, the hardness and strength of the material increased due to the formed stress in the crystal lattice system.

Creep Test Results

Creep tests were performed at 300 ^{o}C and the humidity condition was controlled in the laboratory. These tests took 3000 second and 4800 cycle [41]. The strain that was determined during the creep which is a time dependent deformation process showing the overall effect of stress and temperature.

Creep strain decreased with increasing MWCNTs content. Although at 5% MWCNTs content, the creep strain value is near to the 4% MWCNTs content composite. The life of the 5% MWCNTs reinforced composite is lower than the 4% MWCNTs. In contrast, the creep life is diminished, as it is obvious from the graph 5% MWCNTs reinforced samples. Increasing the MWCNTs decreases the creep strain.

Deformation increases as a function of stress applied under determined experimental conditions due to the amount of CNT entering the diffusion pathway. Hardening occurs as a result of carbon diffusion, thus Ti-6Al-4V/CNT composites hold lower abrupt deformation velocity values. Therefore, the creep velocity values of Ti6Al4V/MWCNTs composites are the same as the lean Ti6Al4 alloys' [3,42].

In addition, although creep life generally increases with MWCNTs content after 4% of MWCNTs creep life decreases. At 5% of MWCNTs significantly lower creep life was obtained when compared with 3 and 4% of MWCNTs. Fig. 8 presents the creep strain in creep test against MWCNTs content in Ti–6Al–4V matrix reinforced with MWCNTs.

Fig. 9 shows that creep life generally increases with MWCNTs content, creep strain decreases with MWCNTs content. Moreover, creep life decreases with MWCNTs content above 4% of MWCNTs. Increasing the CNT decrease the creep displacement. In addition, although creep life generally increases with CNT content after 4% of CNT creep life decreases. At 5% of CNT significantly lower creep life was obtained when compared with 3 and 4% of CNT. As a result, creep life generally increases with MWCNTs content, creep strain decreases with MWCNTs content. Fig. 10 presents that with MWCNTs content, creep life. Moreover, creep life decreases with MWCNTs content above 4% of MWCNTs.

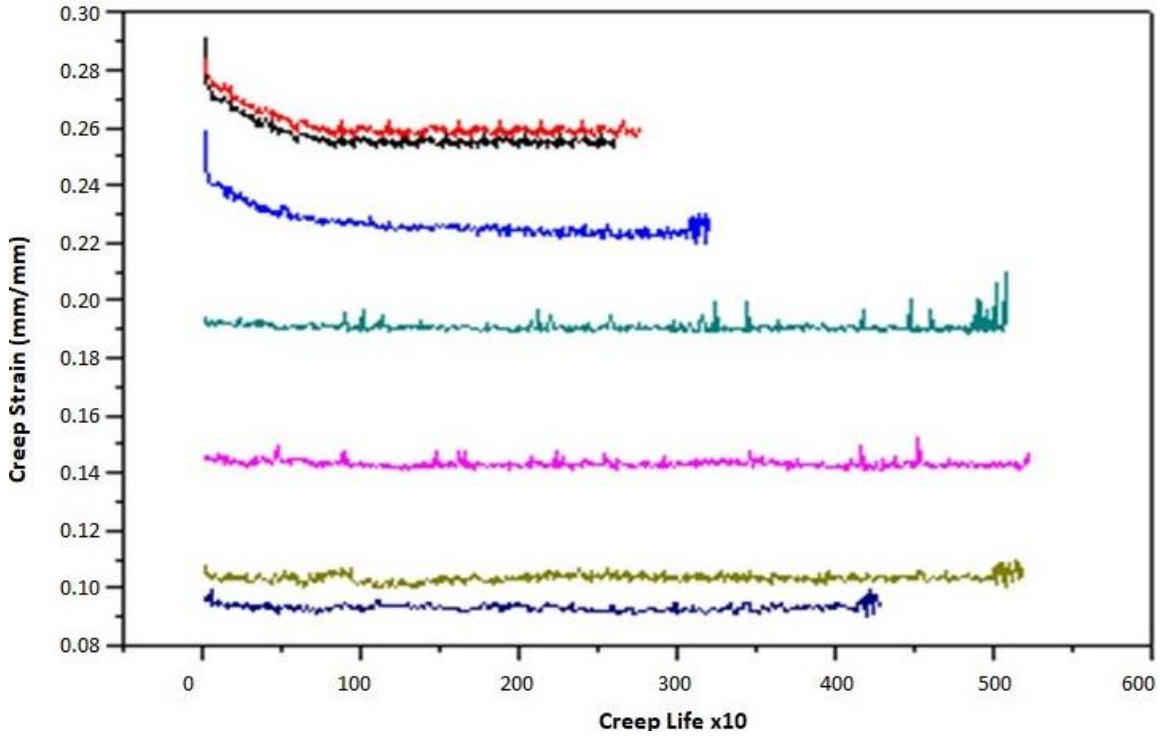

Fig. 9: Static Creep test of the Ti–6Al–4V matrix composites containing different v % MWCNTs.

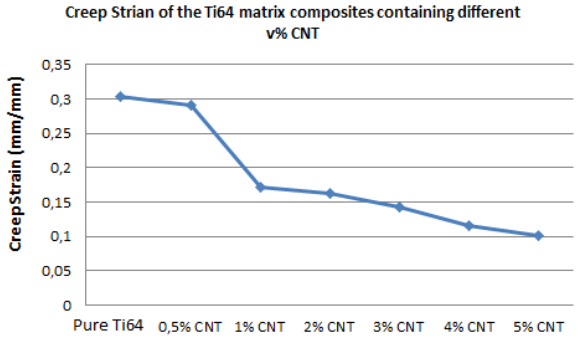

Fig. 10: Static Creep strain of the Ti–6Al–4V matrix composites containing different v % MWCNTs.

The results of the creep test performed under continuous dynamic load for approximately 7 hours are shown in Fig. 9 graphically. After the test, it is clear that non-fast linear deformation occurs in the stable creep zone. The increase in the MWCNT ratio based on this result contributed positively to the creep rate and strain of Ti6Al4V / MWCNT composites. When the related graphs were examined, almost nonlinear deformation occurred in the creep strain which decreased with dynamic stress applied. Stable creep area reached steady state within 60 minutes. Many researchers have assumed that this parameter changes linearly with the carbon content of the carbide. With the same assumption, it is thought that the TiC carbide structure formed in the structure is effective with MWCNT supplementation in our study. MWCNT reinforced materials showed better creep behaviour than pure Ti-6Al-4V material. With the increase of the reinforcement rate, the (TR) carbide structure in the structure may contribute to increase the creep resistance due to the increase of stress in the material [43].

Fig. 11 shows the creep strains against creep life (s) at 300 °C and 400 °C and 300 °C. At 300 °C, the best creep results are obtained for 4% CNT content. Therefore, these samples are also measured at 400 °C and compared with 300 °C. In order for our study to be more meaningful, it is necessary to calculate the activation energy. The equation Eq 2.1 was utilized in this calculation. In this equation, n and A_{ss} constants and in the steady state creep area was used.

$$\dot{\varepsilon}_{ss} = A_{ss}\sigma^{n} \exp\left(\frac{-Q}{RT}\right) Eq.(2.1)[44]$$

The stress value is the one applied to the σ test, the Ass is the equation constant, the temperature is the one applied in the experiment, the stress dependence value of the s strain rate. All of these

data are calculated using the Q activation energy. Steady state creep condition is the basis of many extrapolation approaches.

$$Q = \frac{R \ln(\dot{\varepsilon}_1 / \dot{\varepsilon}_2)}{(1/T_2 - 1/T_1)} \quad Eq(2.2)[44]$$

The terms used in Eq 2.2 are $\dot{\varepsilon}_1$, $\dot{\varepsilon}_2$ creep rates, T_1 and T_2 test temperatures, R = basic gas constant respectively. The activation energy (Q) is obtained as 248.8 KJ / mole K using stable creep data obtained at two different (300 °C and 400 °C) temperatures as shown in Fig. 11 in the activation energy calculation. For different stresses, the steady-state steady-state tension ratios are obtained from Fig. 11 (b). Then the logarithm between the stress logarithm and the stress is plotted in Fig. 11 (b). The slope of the curve line corresponds to n. n, 0.959. Equation (1) is calculated as 1.55 10-13 (100 MPa) [43].

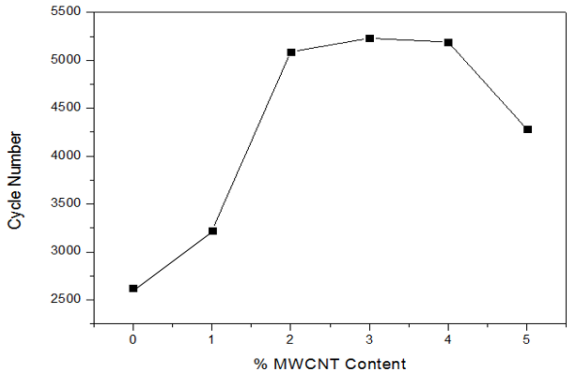

Fig. 11: Creep cycle rate of the Ti–6Al–4V matrix composites containing different v % MWCNTs

In fact comparing to Ref. [44], where creep tests were carried out using cylindrical creep specimens with 39 mm gauge length and 6 mm diameter with 30 kN capacity under constant load in the range from 222 to 300 MPa at 600 ºC, it can be concluded that the creep mechanisms are not only associated with dislocation climbing creep processes but also surface properties of the titanium specimens forming a ceramic titanium oxide corrosion protective layer in contact with atmosphere even after sintering process.

Creep strain decreased with increasing CNT content. Altough at 5% CNT content, the creep strain value is near to the 4% CNT content composite, the life of the 5% CNT reinforced composite is lower than the 4% CNT. The higher amount of carbon content agglomerated and then segregated, thus caused decrease in creep life at 300 ºC These results are parallel to the compression behavior of the composites

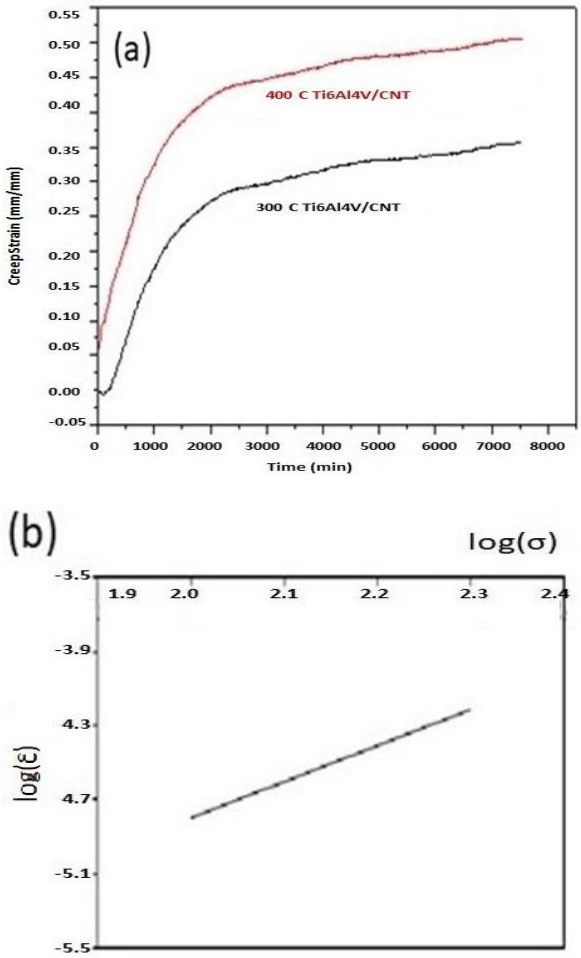

Fig. 12: (a) Strain versus time for 4 % CNT content at 300 oC and 400 oC under 100 MPa, (b) Logarithm of the stress versus logarithm of strain rate.

Conclusion

This work was carried out in order to analyze the effect of MWCNTs addition on the hardness, densification and creep properties of Ti-6Al-4V/MWCNTs composites to shed light on its applicability in several industries where the combination of higher elastical modulus with low density are advantageous.

It has been shown that production of fully dense lightweight Ti-6Al-4V/MWCNTs composites

is possible by means of powder metallurgy technique. At a constant temperature, the density of the sintered composites decreased by an increase in the volume ratio of MWNCTs and this was ascribed to the difficulty to obtain a homogenous distribution of MWCNTs within the matrix. However, microhardness of the sintered samples was enhanced with more MWCNTs addition. This increase in hardness was considered as a result of hard interfacial product TiC.

Ti-6Al-4V/MWCNTs composites can draw attention to creep applications in several industries where the higher temperatures, temperature differences and loading at the mean time are involved during applications. Therefore, this research introduced new prospects for the application of Ti-6Al-4V/MWCNTs composites. All of the sintered samples had α + β microstructure. Formation of TiC increased the hardness value (538 HV) and the short-term creep behavior of the samples was improved with the help of those carburs which give rise to reduction of immediate deformation and steady-state creep rates. Nevertheless, the effect of carburs on the fracture time was not clear which can ascribe to the possible increase in the surface roughness. Disclocation climbing creep process was concluded as the creep mechanism takes place in the present conditions. All samples revealed an αlpha and beta microstructure. A carburized layer, formed by TiC carburizing, increased the hardness value (538 HV). Immediate deformation was decreased and creep rates became steady as the carbide structure enhanced the short-term creep behavior. Nonetheless, the effect of carbide microsturcure to the fracture mechanism was ambiguous, might be also associated with the increment of the surface roughness. In the current creep case, dislocation climbing creep processes might be included in creep mechanisms.

Good mechanical properties of Ti-6Al-4V having TiC confirms the possible potential of this microstructure in order to improve the high-temperature performance of Ti alloys.

Acknowledgements

This work was supported by the Scientific Research Project Program of Marmara University (FEN-K-070317-0107).

References

1. A. J. Jackson, J. Moteff and F. H. Froes, Advanced titanium-alloy department via powder-metallurgy, *J. Met. P*.**31**, 145 (1979).
2. Z. Y. Ma, R. S. Mishra and S. C. Tjong, High-temperature creep behavior of TiC particulate reinforced Ti-6Al-4V alloy composite, *Acta Mater*, **50**, 4293 (2002).
3. A. O. Adegbenjo, A. Babatunde and B. A. Obadele, Densification, hardness and tribological characteristics of MWCNTs reinforced Ti6Al4V compacts consolidated by spark plasma sintering, *J. Alloys and Compounds*, **749**, 818 (2018).
4. L. Wang, Z. B. Lang and H. P Shi, Properties and forming process of prealloyed powder metallurgy Ti-6Al-4V alloy, *Trans. Nonferr. Met. Soc*.,**17**, 639 (2007).
5. J. Q. Jiang, T. S. Lim, Y. J Kim, B. K. Kim and H. S. Chung, In situ formation of TiC-(Ti-6Al-4V) composites, *Materials Science Technology*, **12**, 362 (1996).
6. İ. Topcu, Ph.D. Thesis, *Determination of mechanical properties of ceramic reinforced Al matrix composites under dynamic loading conditıons*, Marmara Universty, (2007).
7. A. G. Mamalis, L. O. G. Vogtländer and A. Markopoulos, Nanotechnology and nanostructured materials trends in carbon nanotubes, *Precision Engineering*, **28**, 16 (2004).
8. E. T. Thostenson, Z. Ren, T. W. Chou, Advances in the science and technology of carbon nanotubes and their composites, *Composites Science and Technology*, **61**, 1899 (2001).
9. A. K. Lau and D. Hui, The revolutionary creation of new advanced materials carbon nanotube composites, *Composite. Part B: Engineering*, **33**, 263 (2002).
10. R. B. Pipes and P. Hubert, Helical carbon nanotube arrays: mechanical properties, *Composites Science and Technology*, **62**, 419 (2002).
11. J. Salvetat-Delmotte and A. Rubio, Mechanical properties of carbon nanotubes: a fiber digest for beginners, *Carbon*, **40**, 1729 (2002).
12. E. Saether, S. J. Frankland, and R. B.Pipes, Self-consistent properties of carbon nanotubes and hexagonal arrays as composite reinforcements, *Composites Science and Technology*. **63**, 1543 (2003).
13. M. Leila and T. V. Mohammad, Solid Phase Extraction and Determination of Methyldopa in Pharmaceutical Samples Using Molecularly Imprinted Polymer Grafted Carbon Nanotubes, *J.Chem.Soc.Pak.* **39**, 446 (2017).
14. A. K.Shukla, N. Nayan, S. V. S. N. Murty, S. C. Sharma, P. Chandren, S. R. Bakshi and K. M. George, Processing of copper carbon nanotube composites by vacuum hot pressing technique,

Materials Science and Engineering A. **560**, 365 (2003).
15. L. Valentini, J. Biagiotti, J. M. Kenny, and S. Santucci, Morphological characterization of single-walled carbon nanotubes-PP composites, *Composites Science and Technology*, **63**, 1149 (2003).
16. W. K. Maser, A. M. Benito, M. A. Callejas, T. Seeger, M. T. Mart´ınez, J. Schreiber, J. Muszynski, O. Chauvet, Z. Osváth, A. A. Koósand L. P Biró, Synthesis and characterization of new polyaniline/nanotube composites, *Mater. Sci. Enginering C.* **23**, 87 (2003).
17. R. Andrews and M. C. Weisenberger, *Carbon nanotube polymer composites*, *Current opinion in solid State Material Sciences*, **8**, 31 (2004).
18. P. M. Ajayan, L. S. Schadler, C. Giannarisand A. Rubio, Synthesis and characterization of plasma spray formed carbon nanotube reinforced aluminum composite, *Adv. Materrials*, **12**, 750 (2002).
19. T. Laha, A. Agarwal, T. McKechnie and S. Seal, Syntesis and characterization of plasma spray formed carbon nanotube reinforced aluminum composite, *Materials Science and Engineering A* **381**, 249 (2004).
20. M. Wong, M. Paramsothy, X. J. Xu, Y. Ren, S. Li, and K. Liao, Physical interactions at carbon nanotube-polymer interface, *Polymer*, **44**, 7757 (2003).
21. G. M. Odegard, R. B. Pipes and P. Hubert, Comparison of two models of SWCN polymer composites, *Composites Science and Technology*, **64**, 1011 (2003).
22. E. Kymakis, I. Alexandou and G. A. J. Amaratunga, Single-walled carbon nanotube-polymer composites: electrical, optical and structural investigation, *Synth. Met.*, **127**, 59 (2002).
23. Z. Balázsi, F. Kónya, L. Wéber, L., Biró, L and P. Arató, Preparation and characterization of carbon nanotube reinforced silicon nitride composites, *Materials Science Engineering C*, **23**, 1133 (2003).
24. S. Khalid and K. Nasib, Preparation, Morphologies and Properties of Multiwalled Carbon Nanotubes-Filled PMMA/PVC Blends, *J. Chem. Soc. Pak*. **37**, 284 (2005).
25. X. Feng, J. Sui, W. Cai and A. Liu, Improving wear resistance of TiNi matrix composites reinforced by carbon nanotubes and in situ TiC, *Scripta Materialia*, **64**, 824 (2011).
26. T. Threrujirapapong, K. Kondoh, J. Umeda and H. Imai, Friction and wear behavior of titanium matrix composite reinforced with carbon nanotubes under dry conditions, *Transactions of JWRI*, **37,** 51 (2008).
27. S. Bakshi, D. Lahiri and A. Agarwal, Carbon nanotube reinforced metal matrix composites, *International Materials Reviews*, **55**, 41 (2010).
28. Z. Abdallah, K. Perkins and S. Williams, Advances in the Wilshire extrapolation technique full creep curve representation for the aerospace alloy titanium, *Mater Sci Eng A*, **550**, 176 (2012).
29. C. J. Boehlert and W. Chen, The elevated-temperature creep behavior of boron-modified Ti-6Al-4V alloys, *Mater Trans.*, **50**, 1690 (2009).
30. F. J. Seco and A. M. Irisarri, Creep failure mechanisms of Ti-6Al-4V thick plate, *Fatigue Fracture Engineerin Materials Structure*, **24**, 741 (2001).
31. C. Suryanarayana, Mechanical alloying and milling, *Progress in Materials Science*, (2001).
32. İ. Topcu, A. N. Güllüoğlu, M. K. Bilici and H. Ö. Gülsoy, Investigation of wear behavior ofTi-6Al-4V/CNT composites reinforced with carbon nanotubes, *J. Faculty of Engineering and Architecture of Gazi University*, **32** (2019).
33. I. Topcu, H. Ö. Gulsoy, N. Kadıoglu and A. N. Gulluoglu, Processing and Mechanical properties of B4C Reinforced Al Matrix Composites, *J. Alloys and Compounds*, **482** , 516 (2009).
34. E. T. Thostenson, Z. Ren and T. W. Chou, Advances in the science and technology of carbon nanotubes and their composites, *Composites Science and Technology*, **61**, 1899 (2001).
35. X. Feng, J. Sui, W. Cai and A. Liu, Improving wear resistance of TiNi matrix composites reinforced by carbon nanotubes and in situ TiC, *Scripta Materialia*, **64**, 824 (2011).
36. W. Cai, X. Feng and J. Sui, Preparation of multi-walled carbon nanotube-reinforced TiNi matrix composites from elemental powders by spark plasma sintering, *Rare Metals*, **31**, 48 (2012).
37. K. S. Munir, Y. Li, D. Liang, M. Qian, W. Xu and C. Wen, Effect of dispersion method on the deterioration, interfacial interactions and re-agglomeration of carbon nanotubes in titanium metal matrix composites, *Materials & Design*, **88**, 138 (2015).
38. K. S. Munir, D. T. Oldfield and C. Wen, Role of Process control agent in the synthesis of multiwalled carbon nanotubes reinforced titanium metal matrix powder mixtures, *Adv. Eng. Mate.*, **18**, 294 (2016).
39. N. Saheb, A. Khalil, A. Hakeem, N. Al-Aqeeli, T. Laoui and A. Qutub, Spark plasma sintering of CNT reinforced Al6061 and Al2124

nanocomposites, *J. Composite Materials*, **18** (2014).

40. A. Peigney, E. Flahaut, C. Laurent, F. Chastel and A. Rousset, Aligned carbon nantubes in ceramic-matrix nano composites prepared by high tempareture extrusion, *Chem. Phys. Lett*., **352**, 20 (2002).
41. F. C. Wang, Z. H. Zhang, Y. J. Sun, Y. Liu, Z. Y. Hu, H. Wang, A. V. Korznikov, E. Korznikova, Z. F. Liu and S. Osamu, Rapid and low temperature spark plasma sintering synthesis of novel carbon nanotube reinforced titanium matrix composites, *Carbon*, **95**, 396 (2015).
42. V. M. Oliveiraa, C. A. Mariane, M. C. L. Silvaa, C. G. Pinto, P. A. Suzuki, J. P. B. Machado and M. J. R. Barbozaa, Short-term creep properties of Ti-6Al-4V alloy subjected to surface plasma carburizing process, *J. Materials Research and Technology*, **4**, 359 (2015).
43. M. J. R. Barboza, E. A. C. Perez, M. M. Medeiros, D. A. P Reis, M. C. A Nono and N. F. Piorino,Creep behavior of Ti-6Al-4V and comparison with titanium matrix composites, *Mater Sci. Eng. A*, **428,** 319 (2006).
44. A. O. Adegbenjo, A. Babatund and B. A. Obadele, Densification, hardness and tribological characteristics of MWCNTs reinforced Ti6Al4V compacts consolidated by spark plasma sintering, *J. Alloys and Compounds*, **749**, 818 (2018).